

**Toxicokinetics and Physiologically Based Pharmacokinetic Modeling of the Shellfish Toxin
Domoic Acid in Nonhuman Primates**

Jing Jing, Rebekah Petroff, Sara Shum, Brenda Crouthamel, Ariel R. Topletz, Kimberly S. Grant,
Thomas M. Burbacher, and Nina Isoherranen

Department of Pharmaceutics, University of Washington, Seattle, Washington, USA (J.J., S.S.,
A.R.T., N.I.)

Department of Environmental and Occupational Health Sciences, University of Washington,
Seattle, Washington, USA (R.P., B.C., K.S.G., T.M.B.)

Center on Human Development and Disability, University of Washington, Seattle, Washington,
USA (B.C., K.S.G., T.M.B. N.I.)

Infant Primate Research Laboratory, Washington National Primate Research Center, Seattle,
Washington, USA (K.S.G., T.M.B.)

Running Title: Toxicokinetics and PBPK Modeling of Domoic Acid in Monkeys

Corresponding author: Nina Isoherranen

Address: University of Washington Health Science Building Room H-272M Box 357610

Seattle, WA 98195-7610

Telephone: (206) 543-2517; Fax: (206) 543-3204; Email: ni2@uw.edu

No. of text pages:

No. of tables: 3

No. of figures: 7

No. of references: 38

Number of words in:

Abstract: 250

Introduction: 750

Discussion: 1469

Abbreviations: AUC, area under the plasma concentration time curve; CL, clearance (CL), C_{max} , maximum plasma concentration; DA, domoic acid; F, bioavailability; k, linear terminal slope; LC-MS/MS, liquid chromatography tandem mass spectrometry; LLOQ lower limit of quantification; NOAEL, no observed adverse effect level; PBPK, physiologically based pharmacokinetic; t_{max} , time to reach C_{max} ; TDI, tolerable daily intake; $t_{1/2}$, half-life; V_{ss} , volume of distribution at steady state; QC, quality control

Abstract

Domoic acid (DA), a neurotoxin, is produced by marine algae and has caused toxications worldwide in animals and humans. However, the toxicokinetics of DA has not been fully evaluated, and information is missing on the disposition of DA following oral exposures at doses that are considered safe for human consumption. In this study, toxicokinetics of DA were investigated in cynomolgus monkeys, following single doses of 5 $\mu\text{g}/\text{kg}$ DA iv, 0.075 mg/kg DA po and 0.15 mg/kg DA po. Following iv dosing, DA had a systemic clearance of 124 ± 71 ml/hr/kg, volume of distribution at steady state of 131 ± 71 ml/kg and elimination half-life of 1.2 ± 1.1 hours. However, following po dosing, the average terminal half-life of DA was 11.3 ± 2.4 hours, indicating that DA disposition follows flip-flop kinetics with slow, rate-limiting, absorption. The absorption of DA was low after po dosing with absolute bioavailability of $7 \pm 4\%$. The renal clearance of DA was variable (21-152 ml/hr/kg) with $42 \pm 11\%$ of the DA iv dose recovered in urine. A physiologically based pharmacokinetic (PBPK) model was developed for DA in monkeys and humans that replicated the flip-flop kinetics observed after oral administration, and allowed simulation of urinary excretion and brain and kidney distribution of DA following iv and po dosing. This study is the first to characterize DA disposition at exposure levels close to the current estimated Tolerable Daily Intake (TDI) and to mechanistically model DA disposition in a model species, providing important information of the toxicokinetics of DA for human safety assessment.

Introduction

Domoic acid (DA, Figure 1) is a neurotoxic kainic acid and glutamate analog that binds to α -amino-3-hydroxy-5-methylisoxazole-4-propionate (AMPA) and kainate receptors, resulting in lesions in the hippocampus and amygdala (Pulido, 2008). DA is produced by several *Pseudo-nitzschia* algal species in seawater (Mos, 2001). As *Pseudo-nitzschia* blooms are initiated by anomalously warm ocean conditions, increasing sea temperatures are predicted to increase algal blooms and consequently DA outbreaks and exposure. Indeed, in 2015 warm ocean conditions resulted in *Pseudo-nitzschia* blooms that led to the largest outbreak of DA along the North American west coast (McCabe *et al.*, 2016). As DA is transferred through marine food webs via ingestion of *Pseudo-nitzschia* cells, and by consumption of the organisms contaminated with DA (Lefebvre *et al.*, 2002; Lefebvre and Robertson, 2010), DA intoxications in marine animals are closely tied to severity of DA producing algal blooms (Scholin *et al.*, 2000; Lewitus *et al.*, 2012; Du *et al.*, 2016). Hence, the increase in DA outbreaks also precipitates a potential increase in public health risks of exposure to DA.

Human DA poisoning affected over 100 individuals in 1987. Three individuals died and others reported signs of DA related amnesic shellfish poisoning including gastrointestinal distress, neurological abnormalities, seizures and autonomic nervous system dysfunction (Perl *et al.*, 1990; Todd, 1993). Analysis of nine of these cases suggested the toxication was due to consumption of DA containing mussels, at intake levels of 60-290 mg (0.9-4.1 mg/kg) of DA (Perl *et al.*, 1990), but DA concentrations in the affected individuals could not be measured. The acute toxicity of DA has since been extensively studied, and oral acute reference doses and Tolerable Daily Intake (TDI) values of 0.018- 0.1 mg/kg have been proposed (Costa *et al.*, 2010). A TDI of 0.075 mg/kg po was suggested based on the no observed adverse effect level (NOAEL) in monkeys following short-

term exposure (0.75 mg/kg/day DA po for 15 days) (Mariën, 1996; Truelove *et al.*, 1997). However, information to establish a chronic TDI for DA is currently not available (Pulido, 2008). Several studies in model species have suggested that chronic low-level DA exposure at asymptomatic doses results in adverse effects including epigenetic changes and sensitization of animals to the toxicity of DA (Hiolski *et al.*, 2014; Lefebvre *et al.*, 2017). Yet, the underlying mechanisms of these changes and DA toxicokinetics at asymptomatic doses have not been characterized. The lack of knowledge of the toxicokinetics of DA is largely due to limited bioanalytical methods to measure DA. LC-MS/MS methods exist for measuring DA in seawater and in contaminated seafood (Wang *et al.*, 2012; Barbaro *et al.*, 2016), but these methods lack the sensitivity needed to quantify DA in biological samples following low level exposure (Frame and Lefebvre, 2013). ELISA can measure DA at concentrations down to 0.4 ng/ml in biological specimens (Frame and Lefebvre, 2013), but the ELISA assay also cross reacts with antibodies against DA, decreasing the usefulness of this assay following chronic exposures (Lefebvre *et al.*, 2012). Therefore, improved LC-MS/MS methods are needed to allow evaluation of DA exposures.

DA is a polar compound ($\log P = -0.23$) with four ionized groups, three carboxylic acids (pK_a 's 1.85-4.75) and an amine (pK_a 10.6) (Walter *et al.*, 1992). Hence, it is expected to have limited permeability across physiological barriers such as intestinal epithelium, blood brain barrier and the placenta. Low permeability of DA in Caco-2 cells has been shown (Kimura *et al.*, 2011) and the bioavailability of DA appears to be low (<10%) based on observed excretion of DA into urine following iv and po doses to monkeys (Truelove and Iverson, 1994; Truelove *et al.*, 1997), and recovery of unchanged DA in feces of rodents after oral dose (Iverson *et al.*, 1990). Distribution of DA to the brain and penetration to the developing fetus in pregnant rodents has also been shown after iv doses to rodents (Maucher-Fuquay *et al.*, 2012a; b). Yet, knowledge of

the overall toxicokinetics and target tissue distribution of DA following exposures similar to those that may occur in humans is lacking.

As human and wildlife exposures to DA are exclusively via oral consumption, the aim of this study was to characterize DA toxicokinetics following oral administration to nonhuman primates at levels of exposure near and at the proposed TDI level, and to establish the key toxicokinetic parameters of DA following iv and po dosing to monkeys. Physiologically based pharmacokinetic (PBPK) models of DA toxicokinetics in monkeys and humans were developed to allow simulation of DA toxicokinetics following different routes of administration after acute and chronic exposure.

Materials and Methods

Chemicals and Reagents. DA was purchased from BioVectra (Charlottetown, PE, Canada). Certified calibration solution for DA was purchased from National Research Council Canada (Ottawa, Ontario, Canada). Optima grade water, methanol, acetonitrile and formic acid used for bioanalytical assays were purchased from Fisher Scientific (Pittsburgh, PA). β -glucuronidase from *E. coli* and ammonium acetate were purchased from Sigma-Aldrich (St. Louis, MO).

Animal Studies. The study was conducted in three healthy adult female cynomolgus monkeys between ages 9.8 and 10.3 years and weighing 5.2 ± 1.6 kg (range 3.5-7.2 kg). Animals were housed in the Infant Primate Research Laboratory at the Washington National Primate Research Center. Animals were unsedated for the duration of the study, with unrestricted access to food and water. Animals were fed with Lab Diet High Protein Monkey Diet biscuits twice a day, once approximately 2 hours before the DA dose and once approximately 5 hours after the dose of DA. All animal procedure guidelines followed the Animal Welfare Act and the Guide for Care and Use of Laboratory Animals of the National Research Council. All protocols were approved by the University of Washington Institutional Animal Care and Use Committee.

A single iv dose of 5 μ g/kg DA dissolved in sterile saline was administered. Blood samples were collected from the saphenous vein before treatment (baseline) and 5, 10, 20, 30 and 45 minutes, and 1, 1.5, 2, 3, and 4 hours after treatment. Two repeated iv studies were conducted in these animals. During the second iv study urine and feces were collected from cage pans after every blood draw during the study period and at 8, 12, and 24 hours post dose. The DA kinetics was also characterized in these animals following a single oral dose of 0.075 mg/kg or 0.15 mg/kg DA. DA oral dose was prepared by dissolving 1 mg/ml DA in tap water with 5% sucrose and the

solution was filtered with syringe filter (0.2 μ M, 25mm) before use. The dose was given to animals without restraint. Blood samples were collected at baseline and at 1, 1.5, 2, 3, 5, 8, 12, 16, 24 and 48 hours post dose. Urine was collected from cage pans after every blood draw for 24 hours during the study with 0.075 mg/kg DA po. A washout period of at least two weeks was given between each exposure.

Blood samples were collected into sodium heparin tubes and centrifuged at 3,000 g for 15 minutes to isolate plasma for further analysis. Plasma, urine and feces samples were stored at -20°C until analysis. For all studies, the dosing solutions were analyzed for DA content by LC-MS/MS as described below to confirm DA concentrations.

DA Plasma Protein Binding and Blood to Plasma Ratio. The protein binding of DA in plasma was determined by ultracentrifugation using plasma samples from 6 female cynomolgus monkeys. Three of these monkeys were dosed with 0.15 mg/kg DA orally, 4-6 hours prior to blood sampling allowing determination of plasma protein binding in exposed animals at physiologically relevant concentration (1 – 10 nM). The other three monkeys were unexposed and the plasma from these animals was spiked with 100 nM DA. Plasma from each animal was aliquoted into 6 tubes with 100 μ l plasma in each tube. Three of these plasma samples were incubated at 37 $^{\circ}\text{C}$ for 90 minutes and meanwhile another three samples were ultracentrifuged at 451,268 g for 90 mins at 37 $^{\circ}\text{C}$. After ultracentrifugation, the supernatant was collected and prepared together with incubated plasma samples using the method described below for LC-MS/MS analysis. The unbound fraction in plasma ($f_{u,p}$) was determined as DA concentration measured in the supernatant divided by the DA concentration in the incubated plasma samples. The protein binding of DA in human plasma at 100 nM DA was determined similarly by ultracentrifugation using pooled plasma from 8 healthy adult subjects.

The blood to plasma concentration ratio of DA was measured as previously described (Jing *et al.*, 2017) in fresh blood from 6 female cynomolgus monkeys. As described above, three monkeys were dosed with DA and blood to plasma concentration ratio was measured in the collected fresh blood, with DA distribution reflecting that obtained after exposure to DA. Fresh blood from the other three unexposed monkeys was spiked with DA to 100 nM final concentration in whole blood. Samples were mixed, aliquoted into four 700 μ L aliquots, and incubated at 37°C for up to 2 hours with aliquots removed at 10 and 30 minutes, 1 hour and 2 hours. At each time point, 60 μ l of blood in triplicate was removed, and protein was precipitated with 60 μ l methanol. Remaining 500 μ l of blood was centrifuged at 1,000 g for 10 minutes at 4°C to pellet red blood cells and isolate plasma. After centrifugation, 60 μ l of plasma was added to 60 μ l of methanol (in triplicate aliquots), the samples prepared as described below and analyzed by LC-MS/MS. The blood to plasma concentration ratio of DA (100 nM) was measured using identical methods in fresh human blood.

Analysis of DA Concentrations in Biological Samples by LC-MS/MS. For DA measurements in plasma, 60 μ l of methanol was added to 60 μ l plasma, and the samples were centrifuged at 16,100 g for 40 minutes, set at 4°C for 30 minutes and centrifuged again at 16,100 g for 30 minutes. The supernatant was collected for analysis. For plasma samples that had concentrations beyond 40 ng/mL based on initial analysis, the supernatant was diluted 2-fold with water for analysis. For DA measurements in urine, 60 μ l of methanol was added to 60 μ l of urine, the samples were centrifuged at 16,100 g for 20 minutes and supernatant was collected and diluted 10-fold with water for analysis. For urine samples that had DA concentrations above the range of standard curves after this dilution, the supernatant was collected and diluted 50-fold with water for analysis. Samples that had undetectable/unquantifiable concentrations with 10-fold dilution were prepared

with addition of 60 μ l of methanol to 60 μ l urine. These samples were analyzed by LC-MS/MS without further dilution. Standard curves were prepared the same way as the urine samples. For DA measurements in feces, 1 g of feces was first homogenized with 3 ml water using Omni tissue homogenizer (Omni International, Kennesaw, GA). After homogenization, 60 μ l of methanol was added to 60 μ l of sample and the mixture centrifuged for 20 minutes at 16,100 g. The supernatant was collected for LC-MS/MS analysis.

Standard curves were prepared using blank monkey plasma spiked with DA at concentrations of 0.6-40 ng/ml (2-128 nM), blank monkey urine spiked to concentrations 16-996 ng/ml (50-3200 nM) of DA, and blank monkey feces spiked to concentrations 6-103 ng/ml (20-332 nM) of DA. A separate plasma standard curve at 6-199 ng/ml (20-640 nM) of DA was prepared for samples exceeding concentrations of 40 ng/ml. These samples were diluted as described above for high concentration samples. In addition, standard curves for urine analysis were prepared at concentrations of 124-3985 ng/ml (400-12,800 nM) for 1:50 dilution and 0.6-40 ng/ml (2-128 nM) for undiluted samples. All standard curves had ≥ 6 concentrations of DA. High, middle and low concentration quality control (QC) samples that were close to the lowest, middle and highest concentration within the standard curve were extracted along with standard curves and also included in all analyses. Low, middle and high QC samples were at DA concentrations of 0.9, 7 and 30 ng/ml (3, 24 and 96 nM) for plasma measurements, 16, 156 and 623 ng/ml (50, 500 and 2000 nM) for urine measurements and 6, 31 and 62 ng/ml (20, 100 and 200 nM) for feces measurements. Uniform weighing was used for all standard curves.

To determine the potential metabolic conjugation of DA in vivo, urine samples were analyzed with and without β -glucuronidase hydrolysis treatment. Briefly, each urine sample was divided into three 200 μ l aliquots. 46.1 μ l ammonium acetate (1 M) and 40 units (U) β -

glucuronidase (6.1 μl of 6.5 U/ μl in 100 mM ammonium acetate) were added to 200 μl urine and incubated at 37°C for 24 hours. To compare with the samples treated with β -glucuronidase, 52.2 μl ammonium acetate (1 M) was added to an additional 200 μl aliquot of the urine sample and incubated at 37°C for 24 hours. To confirm the stability of DA in this assay, 52.2 μl ammonium acetate (1 M) was added to another 200 μl urine sample and stored at -20°C until analysis. After 24 hours, samples were prepared as described above for analysis by LC-MS/MS.

DA concentrations in plasma samples were measured by LC-MS/MS, using AB Sciex 5500 qTrap Q-LIT mass spectrometer (AB Sciex, Foster City, CA) equipped with an Agilent 1290 UHPLC (Agilent, Santa Clara, CA) and a Synergi™ Hydro-RP 100 Å LC Column (2.5 μm , 50 \times 2 mm; Phenomenex). Compound dependent MS parameters used for detection of DA were collision energy 26, collision cell exit potential 10, declustering potential 100 and entrance potential 10. Gradient elution with a flow rate of 0.5 ml/min using (A) water with 0.1% formic acid and (B) 95% acetonitrile with 5% water and 0.1% formic acid was used. The gradient was from an initial 95% A for 1 min to 0% A over 3 min and then to 95% A for 3 min. Analytes were detected using positive ion ESI mode. MS/MS transition monitored for DA was m/z 312.2>266. DA in the dosing solutions and in urine and feces samples was measured by LC-MS/MS, using AB Sciex 4500 mass spectrometer (AB Sciex, Foster City, CA) equipped with a Shimadzu UFLC XR DGU-20A5 (Shimadzu Scientific Instruments, Columbia, MD) and a Synergi™ Hydro-RP 100 Å LC Column (2.5 μm , 50 \times 2 mm; Phenomenex). Compound dependent mass spectrometer parameters used for detection of DA were collision energy 20, collision cell exit potential 10, declustering potential 51 and entrance potential 10. Gradient elution and MS/MS transitions monitored for DA were as described above. Samples were kept in the autosampler at 4 °C and 10 μl of sample was injected for analysis.

Pharmacokinetic Analysis. Pharmacokinetic parameters including area under the plasma concentration time curve (AUC), volume of distribution at steady state (V_{ss}), systemic clearance (CL), half-life ($t_{1/2}$), maximum plasma concentration (C_{max}), time to reach C_{max} (t_{max}), and linear terminal slope (k) were estimated by standard non-compartmental analysis using Phoenix (St. Louis, MO). The geometric mean values are reported for all pharmacokinetic parameters. AUC was determined by the linear log trapezoidal method for iv dosing data and linear trapezoidal method for po dosing data, and extrapolated to infinity using the determined linear terminal slope (from last 5-7 timepoints in iv studies and 3-5 timepoints in po studies) and last observed plasma concentration. Absolute bioavailability (F) was calculated using equation:

$$F = \frac{AUC_{po}}{AUC_{iv}} \times \frac{Dose_{iv}}{Dose_{po}}$$

Renal clearance (CL_R) after iv and po dose was obtained using equation:

$$CL_R = \frac{A_{e,0-24}}{AUC_{0-24}}$$

in which $A_{e,0-24}$ is the amount of DA excreted in urine over 24 hours after iv or po dose and the AUC_{0-24} is the AUC over the 24-hour interval after iv or po dose.

Creatinine clearance (CL_{cr}) in the monkeys was calculated using equation:

$$CL_{cr} = \frac{dA_e}{C \cdot dt}$$

in which A_e is the amount of creatinine excreted in urine over a 4-hour interval (dt) and C is the concentration of creatinine measured in plasma. Blood and urine samples for creatinine clearance measurement were collected before the DA iv dose. Blood and urine creatinine concentrations

were measured by clinical assays at Department of Laboratory Medicine, University of Washington Medical Center.

PBPK Model of DA disposition in Monkeys. A PBPK model of DA was constructed as a full PBPK model using Simcyp Monkey version 16 (Certara, Sheffield, UK). This model is based on cynomolgus monkey physiology without any gender differences in physiological parameters, i.e the simulation results are independent of sex. The absorption kinetics of DA was simulated with advanced dissolution, absorption and metabolism (ADAM) model. In brief, the fraction absorbed (F_a) and F were predicted using mechanistic P_{eff} model with scaling factor of 0.45 applied to the P_{eff} predicted from physicochemical parameters for each part of intestine, to account for the multiple charges in DA molecule that could not be included in the prediction. For DA distribution, a full PBPK model was used. A K_p value for brain was assigned according to the reported AUC_{brain}/AUC_{plasma} ratio in pregnant rats (Maucher-Fuquay *et al.*, 2012a). For kidney, liver and heart, K_p values were estimated based on the reported concentrations in mice (Funk *et al.*, 2014). K_p values for the rest of the organs were independently predicted in Simcyp using the method described by Rodgers and Rowland (Rodgers and Rowland, 2006) with application of a K_p scalar to obtain measured V_{ss} that was consistent with the iv study. The elimination of DA was characterized using the measured systemic clearance after iv dosing (124 mL/hr/kg, range 87 – 218 mL/hr/kg). The geometric mean renal clearance in all the animals in all the study days (59 mL/hr/kg, range 21 – 152 mL/hr/kg) was used in the model. The rest of the systemic clearance (65 mL/hr/kg) was assigned as biliary clearance based on lack of observed metabolism of DA, and the detection of unchanged DA in the feces of monkeys after iv dosing and in bile of marine mammals. It is important to note that it is possible DA is also metabolized, but as the current data cannot differentiate between biliary clearance and metabolism either by gut microbiome or by the monkey

enzymes, only biliary clearance was included to reflect clearance by other pathways. The biliary clearance per hepatocyte was back-calculated using retrograde scaling. The percentage available for reabsorption was set as 100% and a sensitivity analysis was conducted for values between 0 and 100%. The model was found to be insensitive to this value. The details of the model input parameters are listed in Table 1, and representative model output files are included as supplemental data. The model acceptance criterion was set as ≤ 2 -fold difference between the mean simulated values and observed mean values for AUC. The predicted variability in DA disposition was simulated using the range of observed renal clearance values in this study, as the Simcyp monkey model does not allow simulation of population variability in renal or biliary clearance.

The DA PBPK model was tested by simulating DA disposition in monkeys following iv and po dosing, and comparing the simulated results with the in-house toxicokinetic data and the reported data from literature following higher doses of DA to monkeys. In all the simulations renal clearance values were scaled to the reported body weights of the monkeys in the observed studies. The observed concentration–time profiles from prior publications reporting DA plasma concentrations in cynomolgus monkeys (Truelove and Iverson, 1994; Truelove *et al.*, 1997) were digitized using Plot Digitizer software (<http://plotdigitizer.sourceforge.net>). For each study, Simcyp species representative individuals were simulated at fed condition using observed range of renal clearances to represent population variability. Sensitivity analysis was done on biliary clearance ranging from 0.23 to 0.53 $\mu\text{L}/\text{min}/\text{million cells}$, by comparing first order absorption kinetics and ADAM model, and fed and fasted conditions. With the exception of fed versus fasted conditions, the model was found to be sensitive to all of the above parameters.

PBPK Model of DA disposition in Humans. A PBPK model of DA disposition in humans was constructed as a full PBPK model using Simcyp version 16 (Certara, Sheffield, UK). The model

was based on the developed cynomolgus monkey model using body weight scaled physiology, renal clearance and biliary clearance. The absorption kinetics of DA was simulated with human ADAM model. The predicted permeability values corresponded to those used in the monkey model with predicted mechanistic P_{eff} values and the same scaling factor of 0.45. For DA distribution, the K_p values applied to the monkey tissues were also applied in the human model. Both biliary secretion and renal clearance were incorporated in the model. For biliary clearance, the same CL_{int} value in $\mu\text{l}/\text{min}/10^6$ cells was used in the human model and the monkey model. Human renal clearance value was set as 38% of GFR based on the data obtained in the monkeys. No model acceptance criterion was set, as no data exists of DA disposition in humans. DA disposition in humans was simulated in 100 healthy individuals (age: 18 – 65, average body weight: 80.7 kg, 34% female) using the TDI dose (0.075 mg/kg) and the estimated dose range (0.9 – 4 mg/kg) in the Canadian toxication incidence. A representative model output file is included as supplemental data.

Results

Development of a Sensitive and Specific LC-MS/MS Method to Measure DA in Biological

Samples. In order to measure DA in biological samples including plasma and urine following iv and po administration at a dose level near or at the proposed TDI, a sensitive LC-MS/MS method was developed and validated. DA was detected in monkey plasma and urine using this method and the chromatograms of DA in the biological matrices are shown in Figure 2. The assay was validated according to the published guidelines for bioanalytical method validation (Shah *et al.*, 2000; Viswanathan *et al.*, 2007). The lower limits of quantification (LLOQ) in plasma and urine were 0.6 ng/ml (2 nM) and 1.6 ng/ml (5 nM), respectively, based on signal-to-noise ratio >9 and interday CV% < 15%. The accuracy and CV% values of QC samples were <15% at all concentrations. The assay was determined sensitive enough to measure DA concentrations in plasma following oral exposures at the proposed TDI level of DA.

Toxicokinetics of DA Following Single iv and po Doses. The toxicokinetics of DA following iv and po administration was studied in three female monkeys. Following an iv dose of 5 µg/kg DA, DA had a systemic clearance of 124 ± 71 ml/hr/kg (n=6) and a short elimination half-life of 1.2 ± 1.1 hours (Table 2 and Figure 3A). On average, $42 \pm 11\%$ (n=3) of the DA dose was recovered in urine over 24 hours after the iv dose. Based on urinary excretion (Figure 3B), the renal clearance of DA in these animals was 36 ± 30 ml/hr/kg which is 29% of mean systemic clearance and 23% of the creatinine clearance (155 ± 55 ml/hr/kg) in these monkeys. This suggests significant reabsorption of DA in the kidney, and potential other elimination routes of DA including biliary secretion. In accordance with some biliary secretion of DA, DA was also detected in feces after iv dosing at small and variable amounts (data not shown), and the highest DA concentration in feces was 72 ng/g at 0.5 hours post iv dose. Based on DA detection in feces, the maximum total amount

of DA eliminated in 24-hour feces was calculated as 5% of the iv DA dose. Treatment of urine with β -glucuronidase to test potential glucuronidation of DA in vivo did not result in an increase in DA concentration (data not shown).

Administration of a single oral doses of DA to the same monkeys at 0.075 mg/kg and 0.15 mg/kg showed flip-flop kinetics with an absorption rate constant smaller than the elimination rate constant (Figure 3C). Following oral administration of 0.075 mg/kg DA (proposed TDI), maximum DA concentration of 1.5 ± 1.5 ng/ml was reached at approximately 13 ± 5 hours post dose. A maximum DA concentration of 4.5 ± 3.6 ng/ml was reached at 6 ± 2 hours after 0.15 mg/kg oral dose of DA (2-fold of proposed TDI). The terminal half-life of DA was 11.3 ± 2.4 hours and 9.8 ± 5.9 hours following po dosing of 0.075 mg/kg and 0.15 mg/kg DA, respectively (Table 3). Based on the pharmacokinetic analysis, the 8-fold longer half-life after po dosing when compared to iv dosing indicated flip-flop kinetics with elimination rate constant (k) of 0.5 ± 0.2 hr⁻¹ and absorption rate constants (k_a) of 0.06 ± 0.01 hr⁻¹ and 0.07 ± 0.03 hr⁻¹ following 0.075 mg/kg and 0.15 mg/kg oral doses, respectively. The oral clearances of DA were 2.0 ± 0.7 l/hr/kg and 1.6 ± 0.9 l/hr/kg after single oral doses of 0.075 mg/kg and 0.15 mg/kg DA, respectively. Based on the iv and po dosing data, the absolute oral bioavailability of DA was calculated to be 6 ± 4 % and 7 ± 5 % after single doses of 0.075 mg/kg and 0.15 mg/kg DA, respectively. After oral administration of 0.075 mg/kg DA, 4 ± 2 % of the DA dose was recovered in urine over 24 hours (Figure 3D). The renal clearance of DA measured after po dosing was 96 ± 47 ml/hr/kg which was 77% of the systemic clearance of DA after iv dosing (124 ± 71 ml/hr/kg) and 62% of the creatinine clearance (155 ± 55 ml/hr/kg) in these monkeys.

Simulation of DA Disposition in Monkeys Using PBPK Modeling. A PBPK model of DA disposition in monkeys was developed based on obtained experimental and literature data. To

develop the PBPK model, the unbound fraction of DA in plasma and the blood to plasma concentration ratio of DA were measured. No binding of DA was observed in monkey or human plasma and the unbound fraction was determined to be 1.0. Blood to plasma ratio of DA measured in blood from monkeys dosed with DA was 0.59 ± 0.05 . The average hematocrit value for these monkeys was 0.44 ± 0.05 . The blood to plasma ratio measured in spiked blood samples at 100 nM showed consistent values during the time of incubation with average value of 0.56 ± 0.02 . The average hematocrit value for these monkeys was 0.45 ± 0.01 . Blood to plasma ratio of DA measured in human blood showed consistent values during the incubation with average value of 0.51 ± 0.01 . These results indicated no partitioning of DA into red blood cells. As the blood to plasma ratio is dependent on hematocrit of the individual, a blood to plasma ratio of 0.615 was used in the monkey PBPK model based on the defined hematocrit in the monkeys and assuming no blood cell partitioning of DA. The final model parameters are shown in Table 1.

To test the developed DA PBPK model, DA disposition was first simulated in monkeys following administration of single iv doses of 5 $\mu\text{g}/\text{kg}$ and 50 $\mu\text{g}/\text{kg}$ DA, and the simulations were compared to the observed plasma concentration data obtained in this study and in the previously published study (Truelove and Iverson, 1994) (Figure 4A and B, Table 2). The simulated AUC, CL and CL_r were all within 2-fold (between 0.6 and 1.7 – fold) of the observed data in the two iv dosing studies conducted with a 10-fold range in DA doses and in two different laboratories. DA disposition was also simulated in monkeys following single and multiple oral doses using the developed ADAM model for DA absorption. The simulated AUCs for DA all met the acceptance criteria for the model and were within 2-fold (1-1.2 fold) of the observed data after single po doses of 0.075 mg/kg and 0.15 mg/kg DA (Figure 4C and D, Table 3). The PBPK model predicted the flip-flop kinetics of DA with a 12-fold longer simulated half-life after po dosing than after iv

dosing. The predicted terminal half-life (absorption half-life) was within 0.8-fold of the observed. In addition to the current study data, the plasma concentrations of DA following 15 days of oral doses of 0.5 mg/kg/day DA were also simulated in accordance with the dosing in the prior study (Truelove *et al.*, 1997), which measured single time point concentrations of DA following multiple oral doses (Figure 4E). The PBPK model captured the multiple dose pharmacokinetics, predicting the single time point plasma concentrations of DA within the 2-fold criterion (Figure 4E). The simulation accuracy of urinary excretion of DA was also evaluated. The excretion of DA into urine as a function of time was compared to the data collected in this study and in previously reported studies (Figure 5). Overall the mean simulated data of DA dose recovery in urine after both iv and po dosing were within 2-fold of the mean observed data, although inter-individual and inter-day variability within an individual could be over 2-fold in the observed data.

The predominant sites of DA toxicity appear to be the brain and possibly the kidney. Therefore, the concentration-time curves of DA in the brain and kidney were simulated using the developed PBPK model that incorporated the K_p values for brain and kidney estimated from literature tissue partitioning data. As shown in Figure 6A, following a single iv dose of 5 μ g/kg DA, DA is predicted to rapidly distribute into the brain. Following a single po dose of 0.075 mg/kg DA, the maximum concentration in the brain is predicted to be reached 3 hours post dose with prolonged DA exposure in the brain mimicking the flip-flop kinetics observed in plasma. In fact, despite the initial much higher brain concentrations of DA after iv dosing, the simulated brain concentrations of DA at later time points were higher following po dosing than after iv dosing. Similarly, the distribution pattern of DA was also simulated in kidney following iv and po doses (Figure 6B). The kidney concentration-time profiles were similar to those simulated for the brain. High kidney concentrations were reached rapidly following iv dosing and slowly after po dosing,

with prolonged exposure in the kidney after po exposure. Overall, the predicted kidney tissue concentrations were higher than those predicted for the brain. The simulated brain to plasma and kidney to plasma AUC ratios were 0.066 and 0.46, respectively, reflecting the K_p values observed in rodents. To explore the brain concentration versus time profile of DA following dosing that results in signs of toxicity, the brain concentrations of DA were also simulated in monkeys after 0.075 mg/kg iv (Figure 6C). These simulations predicted a peak brain concentration of 41.6 ng/mL and concentrations above 10 ng/mL up to 1 hr. This suggests that in monkeys brain concentrations above 10 ng/mL correspond to acute toxicity, as the vomiting in monkeys after 0.075 mg/kg iv dose of DA was restricted to the first 9-62 minutes after dosing (Truelove and Iverson, 1994).

Simulation of DA Disposition in Humans Using PBPK Modeling

A PBPK model of DA toxicokinetics in humans was developed based on the nonhuman primate model. DA disposition in humans following exposures at the current acute reference dose and at exposures similar to those estimated in the DA outbreak in Canada in 1987, was simulated using the human PBPK model. The variability in DA disposition in human population was simulated using the population variability in Simcyp library. The simulated plasma and brain concentration-time curves are shown in Figure 7. At TDI (0.075 mg/kg PO), the exposure in humans is predicted to be about 30-40% of that observed in monkeys exposed to the same per kg dose. Similar to the monkeys, DA exposure in humans after a po dose was predicted to be prolonged due to the flip-flop kinetics. The brain concentrations of DA in humans were simulated for the doses of 0.9 – 4.1 mg/kg DA corresponding to the estimated consumption in the DA outbreak in Canada (Perl *et al.*, 1990). The predicted brain concentrations ranged from 1.4 ng/mL to 6.6 ng/mL (Figure 7) and were similar (within 0.2-1-fold) to the simulated brain concentrations in monkeys experiencing DA toxicity.

Discussion

Over recent decades, toxic algal blooms have increased resulting in increased risk of DA poisoning in marine mammals and humans who consume contaminated seafood (McCabe *et al.*, 2016). Oral acute reference doses and TDI of DA have been proposed based on toxicity studies in nonhuman primates and an estimated lowest observed adverse effect levels (LOAEL) in humans (Costa *et al.*, 2010). However, these values were derived without knowledge of DA concentrations in humans, or characterization of the absorption kinetics of DA in humans or nonhuman primates after oral doses. This lack of information is largely due to the limited number of bioanalytical methods to measure DA at low levels in biological samples. In fact, the only plasma concentrations available in a model species after oral exposure are from monkeys dosed at 0.5-0.75mg/kg/day po (Truelove *et al.*, 1997, Figure 4). In rats, after oral administration, DA plasma concentrations were below the LLOQ in all samples analyzed (Iverson *et al.*, 1990; Truelove *et al.*, 1996). Existing LC-MS/MS methods lack sufficient sensitivity (LLOQ>7ng/ml) compared with ELISA (LLOQ=0.4ng/ml) (Frame and Lefebvre, 2013), and require large sample volumes (>500 μ l) (Wang *et al.*, 2012). To allow quantification of DA in biological samples following po doses similar to current NOAEL doses, we developed an LC-MS/MS method with sensitivity similar to the ELISA. This method will be useful for future evaluation of DA kinetics and exposures in experimental animals, wildlife and in humans consuming potentially contaminated seafood.

This study provides the first characterization of the absorption kinetics of DA following oral exposure in mammals, and shows that DA is subject to pronounced flip-flop kinetics with a slow absorption from the gut. Due to the flip-flop kinetics, the terminal half-life of DA following oral exposure is prolonged when compared to what would have been expected from the iv data. The bioavailability of 7% determined in this study, is in excellent agreement with the previous

work suggesting <10 % bioavailability of DA (Truelove and Iverson, 1994; Truelove *et al.*, 1997). This low bioavailability is consistent with the high polarity and fully charged state of DA at physiological pH (Vera-avila *et al.*, 2011), and possible predominantly para-cellular absorption of DA. The extent of absorption and the flip-flop kinetics of DA following po dosing were predicted using the P_{eff} value for DA and the monkey ADAM model in Simcyp. As the mechanistic absorption model predicted DA absorption kinetics in monkeys, a DA PBPK model was developed to predict DA toxicokinetics in humans. The PBPK model predicted flip-flop kinetics for DA also in humans suggesting a prolonged exposure to DA after consumption of contaminated seafood. Yet, it is likely that uptake and efflux transporters contribute to DA absorption kinetics, which is not captured in the current model. In a prior study apical-to-basolateral transport of DA in Caco-2 cells was shown to be decreased by 31.5% when DA was incubated with probenecid (100 mM), a non-specific inhibitor of anion transport (Kimura *et al.*, 2011), suggesting transporter involvement in the intestinal absorption of DA.

The developed monkey PBPK model was also used to simulate the brain and kidney concentrations of DA following iv and po doses of DA. DA concentrations have been previously reported in the kidney, liver, heart and hippocampus of mice (Funk *et al.*, 2014), and in brain and cerebrospinal fluid in pregnant rats (Maucher-Fuquay *et al.*, 2012a). The simulated brain and kidney distribution in monkeys is in excellent agreement with prior data from rats showing rapid distribution of DA into tissues after iv dosing (Maucher-Fuquay *et al.*, 2012a). The simulated fast distribution to the brain is also in agreement with the fast onset of vomiting (2-14 minutes) in monkeys dosed with 50 $\mu\text{g}/\text{kg}$ iv and the duration of the vomiting restricted to the first 9-62 minutes after iv dosing (Truelove and Iverson, 1994). The simulated brain concentration-time curves after oral exposure in either monkeys or humans (Figure 6 and 7) provides insight into the

prolonged onset of signs of DA toxicity following consumption of contaminated mussels by humans. In the 1987 DA outbreak, the onset for symptoms after consumption of DA contaminated mussels was between 15 minutes and 38 hours (median 5.5 hours) (Perl *et al.*, 1990). As shown in Figures 6 and 7, following consumption of DA, the time to reach maximum DA concentrations in the brain is expected to be delayed. The PBPK models predicted similar (within 1-5 fold) peak brain DA concentrations in the human poisoning event and in monkeys dosed iv and experiencing DA toxicity. The PBPK models also predicted a much longer duration of exposure in the brain following po dosing than what is observed after iv dosing. This may be important for chronic toxicity of asymptomatic exposures to DA, that lead to the reported sensitization to DA and to epigenetic changes (Hiolski *et al.*, 2014; Lefebvre *et al.*, 2017). However, the current model does not incorporate possible transporter contributions to brain distribution of DA which requires further study. The DA analogs kainic acid and dehydrokainic acid have been shown to have low blood brain barrier permeability but not require active transport for uptake to the brain (Gynther *et al.*, 2014). Efflux transporters, such as MRP5 may, however, restrict brain exposure to DA and cause some species differences in brain distribution, as DA and kainic acid have been shown to be substrates for MRP5 (Jansen *et al.*, 2015).

Majority of DA clearance is believed to be via the kidney because in rats DA is entirely eliminated via the kidney through glomerular filtration (Suzuki and Hierlihy, 1993). Hence, renal impairment has been considered in estimating human safety factors for DA. However, the data presented here and the previous study in cynomolgus monkeys (Truelove and Iverson, 1994) show less than complete urinary recovery (42-71%) of DA. This suggests that other elimination pathways of DA exist besides renal excretion. Biliary secretion by efflux transporters likely contributes to DA clearance. DA was detected in fecal samples in this study after iv dosing, and

DA has been found in the bile of California sea lions (15- 344.7ng/ml DA) and harbor porpoise (11.7ng/ml DA) (Rust *et al.*, 2014). In addition, consistent with biliary secretion of DA, the plasma-concentration time curves of DA following oral dosing to monkeys had a characteristic second peak for DA concentrations (around 16-24 hours in Figure 3C) suggesting some extent of enterohepatic recycling. In rats, probenecid caused a significant increase in plasma DA levels (Robertson *et al.*, 1992) but had no effect on DA renal clearance (Suzuki and Hierlihy, 1993). In mice, probenecid also increased DA concentrations in kidney tissue and serum (Funk *et al.*, 2014). These findings are consistent with hepatic interaction between probenecid and efflux transporters responsible for DA excretion. Further studies are needed to evaluate the quantitative significance of biliary secretion and possible metabolism in DA clearance, and to identify potential transporters responsible for biliary secretion of DA.

The overall renal clearance of DA in monkeys was lower than the GFR suggesting that, in addition to glomerular filtration, significant DA reabsorption occurs. Due to its high charge state and polarity, passive transcellular reabsorption of DA in the kidney tubule is not expected. Indeed, the renal clearance of DA in the rat has been shown to be similar to the GFR (Suzuki and Hierlihy, 1993). The observation of significant reabsorption of DA in monkeys is consistent with the previous findings after iv dosing of DA to monkeys (Truelove and Iverson, 1994). These data suggest that active transport contributes to the reabsorption of DA in monkeys. As the identity and quantitative importance of specific transporters in DA renal clearance is not known, the observed renal clearance of 1.15mL/min/kg in monkeys was used for the PBPK model. Although the renal clearance and urinary excretion of DA had high inter- and intra-individual variability, the developed monkey PBPK model predicted the urinary excretion of DA following iv and po dosing and single and multiple dose exposures across studies (Figure 5).

In conclusion, this study shows that DA has pronounced flip-flop kinetics in monkeys following oral dosing resulting in lower peak concentrations and longer exposures than would be expected based on iv kinetics and with rapid absorption. The toxicokinetic data together with the PBPK model strongly suggest that efflux transporters in the liver are an important contributor to DA elimination. The developed PBPK model provides a powerful tool for future evaluation of DA disposition in acute and chronic toxicology studies and a framework for future exploration of contribution of transporters to DA clearance and distribution to target organs. The monkey PBPK model also provided a basis for a DA PBPK model in humans, to support extrapolation of toxicity data between species and exposure levels. The results of this study provide important new information to evaluate exposure-toxicity relationships of DA to aid in assessment of human DA exposure risks in different populations.

Acknowledgments

The authors wish to thank Courtney Stanley, Caroline Kenney and the staff at the Infant Primate Research Laboratory and the UW National Primate Research Center for their help in conducting this project.

Authorship Contribution

Participated in research design: Jing, Petroff, Crouthamel, Grant, Burbacher, Isoherranen

Conducted experiments: Jing, Shum, Petroff, Crouthamel, Topletz,

Performed data analysis: Jing, Shum, Topletz, Burbacher, Isoherranen

Wrote or contributed to the writing of the manuscript: Jing, Petroff, Shum, Grant, Burbacher,
Isoherranen

References

- Barbaro E, Zangrando R, Barbante C, and Gambaro A (2016) Fast and Sensitive Method for Determination of Domoic Acid in Mussel Tissue. *Sci World J* **2016**:1–6.
- Costa LG, Giordano G, and Faustman EM (2010) Domoic acid as a developmental neurotoxin. *Neurotoxicology* **31**:409–423.
- Du X, Peterson W, Fisher J, Hunter M, and Peterson J (2016) Initiation and development of a toxic and persistent Pseudo-nitzschia bloom off the Oregon coast in spring/summer2015. *PLoS One* **11**.
- Frame E, and Lefebvre K (2013) *ELISA Methods for Domoic Acid Quantification in Multiple Marine Mammal Species and Sample Matrices*.
- Funk JA, Janech MG, Dillon JC, Bissler JJ, Siroky BJ, and Bell PD (2014) Characterization of Renal Toxicity in Mice Administered the Marine Biotoxin Domoic Acid. *J Am Soc Nephrol* 1–11.
- Gynther M, Petsalo A, Hansen SH, Bunch L, Pickering DS (2015) Blood-Brain Barrier Permeability and brain Uptake Mechanism of Kainic Acid and Dehydrokainic Acid *Neurochem Res.* 542-549.
- Hiolski EM, Kendrick PS, Frame ER, Myers MS, Bammler TK, Beyer RP, Farin FM, Wilkerson H, Smith DR, Marcinek DJ, and Lefebvre KA (2014) Chronic low-level domoic acid exposure alters gene transcription and impairs mitochondrial function in the CNS. *Aquat Toxicol* **155**:151–159.

- Iverson F, Truelove J, Tryphonas L NE (1990) The toxicology of domoic acid administered systemically to rodents and primates. *Can Dis Wkly Rep* **16**:Suppl 1E:15-8; discussion 18-9.
- Jansen RS, Mahakena S, de Haas M, Borst P, van de Wetering K (2015). ATP-binding Cassette Subfamily C Member 5 (ABCC5) Functions as an Efflux Transporter of Glutamate Conjugates and Analogs. *J Biol Chem* **290**:30429-30440.
- Jing J, Nelson C, Paik J, Shirasaka Y, Amory JK, and Isoherranen N (2017) Physiologically Based Pharmacokinetic Model of All- *trans* -Retinoic Acid with Application to Cancer Populations and Drug Interactions. *J Pharmacol Exp Ther* **361**:246–258.
- Kimura O, Kotaki Y, Hamaue N, Haraguchi K, and Endo T (2011) Transcellular transport of domoic acid across intestinal Caco-2 cell monolayers. *Food Chem Toxicol* **49**:2167–2171.
- Lefebvre KA, Bargu S, Kieckhefer T, and Silver MW (2002) From sanddabs to blue whales: the pervasiveness of domoic acid. *Toxicol* **40**:971–977.
- Lefebvre KA, Frame ER, Gulland F, Hansen JD, Kendrick PS, Beyer RP, Bammler TK, Farin FM, Hiolski EM, Smith DR, and Marcinek DJ (2012) A Novel Antibody-Based Biomarker for Chronic Algal Toxin Exposure and Sub-Acute Neurotoxicity. *PLoS One* **7**:e36213, The University of Southern Mississippi.
- Lefebvre KA, Kendrick PS, Ladiges W, Hiolski EM, Ferriss BE, Smith DR, and Marcinek DJ (2017) Chronic low-level exposure to the common seafood toxin domoic acid causes cognitive deficits in mice. *Harmful Algae* **64**:20–29.
- Lefebvre KA, and Robertson A (2010) Domoic acid and human exposure risks: A review. *Toxicol* **56**:218–230.

- Lewitus AJ, Horner RA, Caron DA, Garcia-Mendoza E, Hickey BM, Hunter M, Huppert DD, Kudela RM, Langlois GW, Largier JL, Lessard EJ, RaLonde R, Jack Rensel JE, Strutton PG, Trainer VL, and Tweddle JF (2012) Harmful algal blooms along the North American west coast region: History, trends, causes, and impacts. *Harmful Algae* **19**:133–159.
- Mariën K (1996) Establishing tolerable dungeness crab (*Cancer magister*) and razor clam (*Siliqua patula*) domoic acid contaminant levels. *Environ Health Perspect* **104**:1230–1236.
- Maucher-Fuquay J, Muha N, Wang Z, and Ramsdell JS (2012a) Elimination kinetics of domoic acid from the brain and cerebrospinal fluid of the pregnant rat. *Chem Res Toxicol* **25**:2805–2809.
- Maucher-Fuquay J, Muha N, Wang Z, and Ramsdell JS (2012b) Toxicokinetics of domoic acid in the fetal rat. *Toxicology* **294**:36–41.
- McCabe RM, Hickey BM, Kudela RM, Lefebvre KA, Adams NG, Bill BD, Gulland FMD, Thomson RE, Cochlan WP, and Trainer VL (2016) An unprecedented coastwide toxic algal bloom linked to anomalous ocean conditions. 366–376.
- Mckibben SM, Peterson W, Wood AM, Trainer VL, Hunter M, and White AE (2017) Climatic regulation of the neurotoxin domoic acid. **114**.
- Mos L (2001) Domoic acid: a fascinating marine toxin. *Environ Toxicol Pharmacol* **9**:79–85.
- Perl TM, Bédard L, Kosatsky T, Hockin JC, Todd EC, and Remis RS (1990) An outbreak of toxic encephalopathy caused by eating mussels contaminated with domoic acid. *N Engl J Med* **322**:1775–80, Massachusetts Medical Society.

Pulido OM (2008) Domoic acid toxicologic pathology: A review. *Mar Drugs* **6**:180–219.

Robertson H, Renton K, Kohn J, and White T (1992) Patterns of Fos Expression Suggest Similar Mechanisms of Action for the Excitotoxins Domoic and Kainic Acid. *Ann N Y Acad Sci* **648**:330–334.

Rodgers T, and Rowland M (2006) Physiologically based pharmacokinetic modelling 2: predicting the tissue distribution of acids, very weak bases, neutrals and zwitterions. *J Pharm Sci* **95**:1238–57.

Rust L, Gulland F, Frame E, and Lefebvre K (2014) Domoic acid in milk of free living California marine mammals indicates lactational exposure occurs. *Mar Mammal Sci* **30**:1272–1278.

Scholin CA, Gulland F, Doucette GJ, Benson S, Busman M, Chavez FP, Cordaro J, DeLong R, De Vogelaere A, Harvey J, Haulena M, Lefebvre K, Lipscomb T, Loscutoff S, Lowenstine LJ, Marin R, Miller PE, McLellan WA, Moeller PD, Powell CL, Rowles T, Silvagni P, Silver M, Spraker T, Trainer V, and Van Dolah FM (2000) Mortality of sea lions along the central California coast linked to a toxic diatom bloom. *Nature* **403**:80–84.

Shah VP, Midha KK, Findlay JW, Hill HM, Hulse JD, McGilveray IJ, McKay G, Miller KJ, Patnaik RN, Powell ML, Tonelli A, Viswanathan CT, and Yacobi A (2000) Bioanalytical method validation — A revisit with a decade of progress. *Pharm Res* **17**:1551–1557.

Suzuki CA, and Hierlihy SL (1993) Renal clearance of domoic acid in the rat. *Food Chem Toxicol* **31**:701–706.

Todd E (1993) Domoic acid and amnesic shellfish poisoning - a review. *J Food Prot* **56**:69–83.

Truelove J, Mueller R, Pulido O, and Iverson F (1996) Subchronic toxicity study of domoic acid in the rat. *Food Chem Toxicol* **34**:525–529.

Truelove J, Mueller R, Pulido O, Martin L, Fernie S, and Iverson F (1997) 30-day oral toxicity study of domoic acid in cynomolgus monkeys: Lack of overt toxicity at doses approaching the acute toxic dose. *Nat Toxins* **5**:111–114.

Truelove J and Iverson F (1994) Serum domoic acid clearance and clinical observations in the cynomolgus monkey and Sprague-Dawley rat following a single i.v. dose. *Bull Env Contam Toxicol* **52**:479–86.

Vera-avila LE, Marín-pérez DY, and Covarrubias-herrera R (2011) Trace Level Determination of Domoic Acid in Seawater by Off-line / on-line Solid-phase Extraction Coupled to HPLC-UV. *J Mex Chem Soc* **55**:65–71.

Viswanathan CT, Bansal S, Booth B, DeStefano AJ, Rose MJ, Sailstad J, Shah VP, Skelly JP, Swann PG, and Weiner R (2007) Quantitative bioanalytical methods validation and implementation: Best practices for chromatographic and ligand binding assays. *Pharm Res* **24**:1962–1973.

Walter JA, Leek DM, and Falk M (1992) NMR study of the protonation of domoic acid. *Can J Chem* **70**:1156–1161.

Wang Z, Maucher-Fuquay J, Fire SE, Mikulski CM, Haynes B, Doucette GJ, and Ramsdell JS (2012) Optimization of solid-phase extraction and liquid chromatography-tandem mass spectrometry for the determination of domoic acid in seawater, phytoplankton, and mammalian fluids and tissues. *Anal Chim Acta* **715**:71–79, Elsevier B.V.

Footnotes

This work was supported by grants from the US National Institutes of Health [R01 ES023043], [P51 OD010425] and [HD083091]

Legends for Figures

Figure 1. Structures of domoic acid, kainic acid and glutamic acid.

Figure 2. Detection of domoic acid (DA) by LC-MS/MS in monkey plasma and urine samples.

(A) Blank plasma, (B) Plasma sample spiked with 0.6 ng/ml (2.0 nM) DA, (C) Detection of DA in a plasma sample collected 24 hours after dosing with 0.15 mg/kg DA orally. The detected concentration of DA is 2.0 ng/ml (6.3 nM), (D) Blank urine, (E) Detection of DA in a urine sample spiked with 1.6 ng/ml (5.0 nM) DA, (F) Detection of DA in a urine sample collected 24 hours after a 0.15 mg/kg DA dose po. The concentration of DA is 3.7 ng/ml (11.8 nM). Samples were prepared and analyzed as described in materials and methods.

Figure 3. Toxicokinetics of DA in monkeys (n=3) following iv and po administration.

(A) Mean plasma concentration-time profile of DA following a single iv dose of 5 μ g/kg DA. Each data point represents the mean and standard deviation of the plasma concentrations measured in two different studies in three animals. (B) Time course of DA excretion into urine following iv dosing. The percentage of the iv dose of DA (5 μ g/kg) excreted in the urine as a function of time is shown. Each data point is the mean and standard deviation of three animals. (C) Mean plasma concentration versus time curves of DA following a single oral dose of 0.075 mg/kg and 0.15 mg/kg DA. Each data point represents the mean and standard deviation of 3 monkeys. (D) Time course of DA excretion into urine following po dose of 0.075 mg/kg DA. The percentage of oral DA dose excreted in the urine as a function of time is shown as mean and standard deviation of 3 animals.

Figure 4. Predicted and observed plasma concentration–time profiles of DA in monkeys. The solid line in each panel depicts the mean simulated concentrations of DA, the dashed lines depict the variability estimated from the observed range of renal clearances, and the black circles show the observed data. The simulated doses were 5 $\mu\text{g}/\text{kg}$ DA iv (A), (B) 50 $\mu\text{g}/\text{kg}$ DA iv (Truelove and Iverson, 1994) (B), 0.075 mg/kg DA po (C), 0.15 mg/kg DA po, (D) and 0.5 mg/kg/day DA po for 15 days. (Truelove et al., 1997) (E). Asterisk (*) in panel B denotes timepoints in which the plasma concentration in two animals was reported to be below detection and hence not reported. Asterisk (*) in panels C and D indicates a timepoint in which DA concentration in one animal was below detection limit and hence data for this animal is not shown.

Figure 5. Predicted and observed time course of DA excretion into urine in monkeys following iv and po dosing. The solid line in panels a-c represents the simulated mean, population representative, cumulative % of the administered dose excreted in urine. The dashed lines in each panel show the simulated range of cumulative % of the administered dose excreted based on variability in renal clearance. The black circles show the observed data from the current study (A and C, 5 $\mu\text{g}/\text{kg}$ DA iv and 0.075 mg/kg DA po, respectively) and from previous 50 $\mu\text{g}/\text{kg}$ DA iv (Truelove and Iverson, 1994) (B) and 0.5 mg/kg/day DA po studies (Truelove et al., 1997) (D). In panel D the % of the oral dose excreted into urine over the dosing interval (24 hours) is shown following daily dosing of DA for 15 days. The solid line shows the predicted population representative % of the administered dose excreted into urine over a dosing interval at steady state and the dashed lines show the predicted range at steady state. The mean observed values for cumulative % excreted in urine were 42% in (A) 71% in (B) 4% in (C) and 6% in (D). In comparison, the simulated % excreted in urine were 47% in (A) 47% in (B) 3.5% in (C) and 3.5% in (D).

Figure 6. Simulated concentration–time profiles of DA in monkey brain and kidney. Panel A shows the predicted brain concentration versus time curves for DA following 0.005 mg/kg IV (dashed line) and 0.075 mg/kg PO (solid line) doses of DA. Panel B shows the predicted kidney concentration versus time curves for DA following 0.005 mg/kg IV (dashed line) and 0.075 mg/kg PO (solid line) doses of DA. Panel C shows the predicted brain concentration versus time curve for DA following 0.05 mg/kg IV dose of DA. Areas under the concentration curves (AUC) are shown for each simulation. Predicted C_{\max} values were (A) 4.2 ng/mL and 0.3 ng/mL following IV and PO doses, respectively, (B) 32 ng/mL and 2.0 ng/mL following IV and PO doses, respectively and (C) 41.6 ng/mL following IV dose of DA.

Figure 7. Simulated concentration–time profiles of DA in humans. Panels A and C show the predicted plasma (A) and brain (C) concentration versus time curves for DA following consumption of 0.075 mg/kg of DA. Panel B and D show the predicted plasma (B) and brain (D) concentration versus time curves for DA following consumption of 0.9 mg/kg to 4.1 mg/kg of DA, the exposure estimated in the DA toxification incident. (Dotted lines depict the 95th and 5th percentile obtained from the virtual population) Area under the curve (AUC) are reported in each respective panel. Predicted C_{\max} are (A) 1.8 ng/mL, (B) 21.8 ng/mL and 99.3 ng/mL following 0.9 mg/kg and 4.1 mg/kg of DA doses, respectively, (C) 0.1 ng/mL, (D) 1.4 ng/mL and 6.6 ng/mL following 0.9 mg/kg and 4.1 mg/kg of DA doses, respectively.

Table 1. Summary of input parameter values for DA PBPK model in monkeys

Parameters	Input values	Reference/comment
Molecular weight (g/mol)	311.33	PubChem
logP _{o:w}	-0.23	Drug bank
Compound type	Ampholyte	
pK _a 1	4.75	Walter et al., 1992
pK _a 2	10.6	Walter et al., 1992
Blood-to-plasma ration	0.615	Simcyp default value
f _{u,p}	1.0	Measured
Absorption	ADAM	
F _a	0.07	Predicted
P _{eff} (10 ⁻⁴ cm/s)	0.018	Predicted
f _{u,gut}	1	Predicted
Distribution	Full PBPK model	
V _{ss} (l/kg)	0.15	Measured
K _p – brain	0.066	Maucher-Fuquay et al., 2012a
K _p – kidney	0.46	Funk et al., 2014
K _p – liver	0.13	Funk et al., 2014
K _p – heart	0.05	Funk et al., 2014
K _p – adipose	0.04	Predicted
K _p – bone	0.13	Predicted
K _p – gut	0.17	Predicted
K _p – lung	0.18	Predicted
K _p – muscle	0.17	Predicted
K _p – skin	0.14	Predicted
K _p – spleen	0.17	Predicted
K _p scalar	0.23	Assigned
Elimination		
Renal clearance (ml/min/kg)	1.15	Measured
CL _{int} (Hep) μl/min/10 ⁶ cells ^a	0.53	Assigned (back-calculated from nonrenal clearance)

^aThis value is used to reflect biliary secretion of DA in hepatocytes based on predicted in vivo biliary clearance of 65mL/hr/kg. The model cannot differentiate possible metabolism and biliary secretion and this value should be considered as clearance via other pathways.

Table 2. Observed and predicted toxicokinetic parameters of DA in monkeys after single iv doses. Values are reported as geometric mean \pm S.D. the predicted population representative value is shown together with the predicted range of values included in brackets.

PK parameter	Observed 5 μ g/kg iv	Predicted 5 μ g/kg iv	^a Observed i.v. 50 μ g/kg	Predicted i.v. 50 μ g/kg
AUC _{0-∞} (hr*ng/ml)	40 \pm 24	40 (23 - 58)	700 \pm 334	403 (230 - 578)
CL (ml/hr/kg)	124 \pm 71	124 (87 - 218)	73 \pm 33	124 (87 - 218)
CL _r (mL/hr/kg)	36 \pm 30	59 (21 - 152)	56 \pm 35	59 (21 - 152)
t _{1/2} (hr)	1.2 \pm 1.1	0.8 (0.5 - 1.2)	1.7 \pm 1.0	0.8 (0.5 - 1.2)
V _{ss} (ml/kg)	131 \pm 71	149	165 \pm 17	149

^aData from Truelove and Iverson.,1994.

Table 3. Observed and predicted toxicokinetic parameters of DA in monkeys after single po doses. Values are reported as geometric mean \pm S.D. the predicted population representative value is shown together with the predicted range of values included in brackets.

PK parameter	Observed 0.075 $\mu\text{g/kg po}$	Predicted 0.075 $\mu\text{g/kg po}$	Observed 0.15 $\mu\text{g/kg po}$	Predicted 0.15 $\mu\text{g/kg po}$
AUC _{0-∞} (hr*ng/ml)	39 \pm 14	45 (25 - 66)	93 \pm 45	90 (51 - 132)
C _{max} (ng/mL)	1.5 \pm 1.5	4.4 (2.8 - 5.7)	4.5 \pm 3.6	8.8 (5.6 - 11.5)
t _{1/2} (hr)	11.3 \pm 2.4	9.3 (9.1 - 9.5)	9.8 \pm 5.9	9.3 (9.1 - 9.5)
F (%)	6 \pm 4	7.5	8 \pm 5	7.5

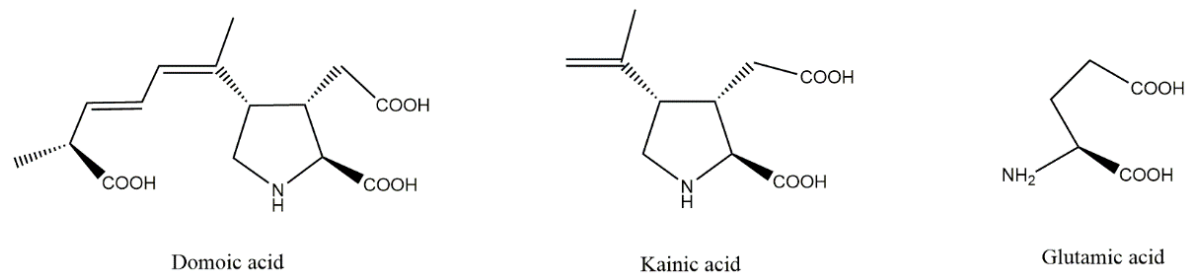


Figure 1.

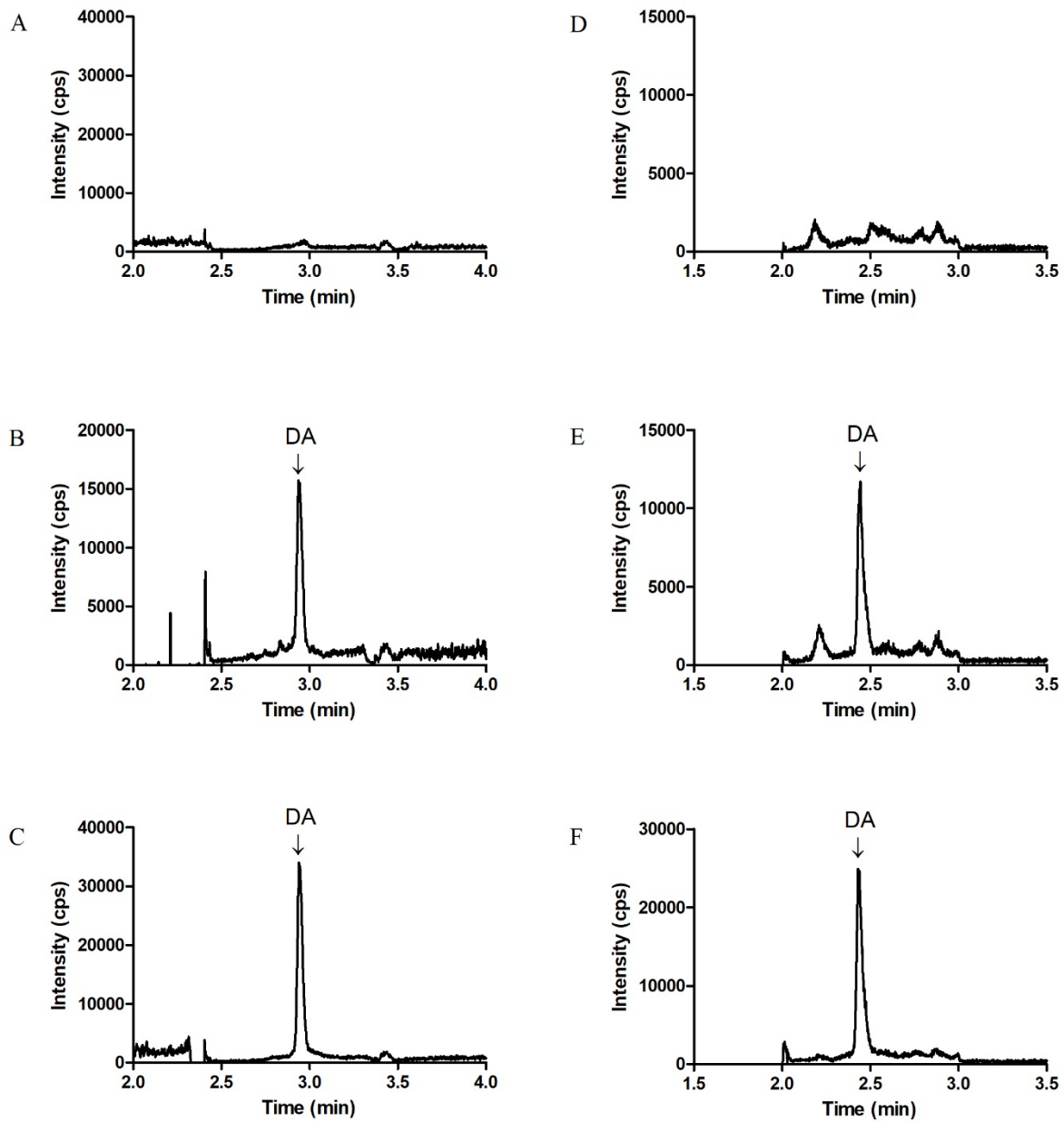


Figure 2.

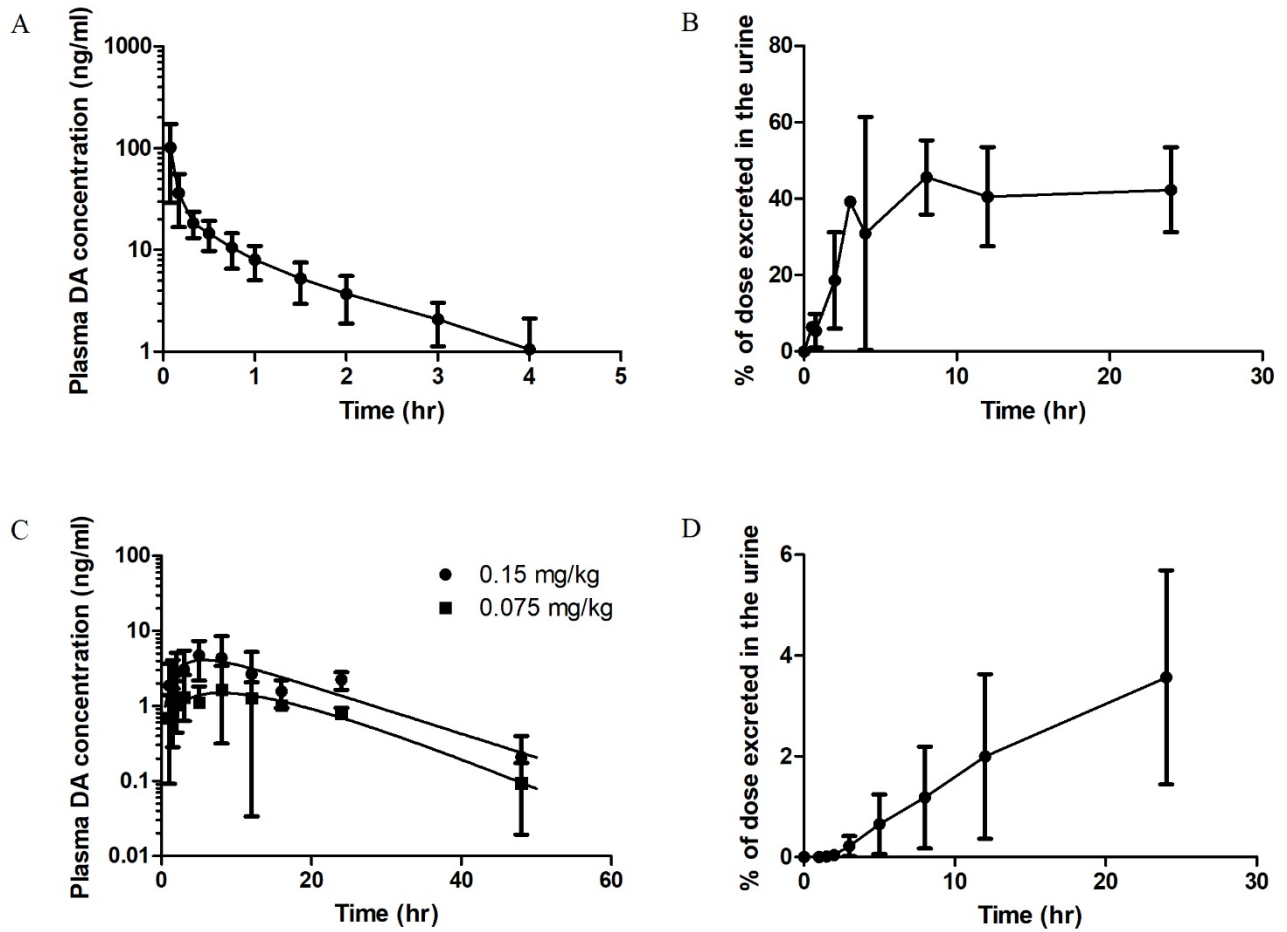


Figure 3.

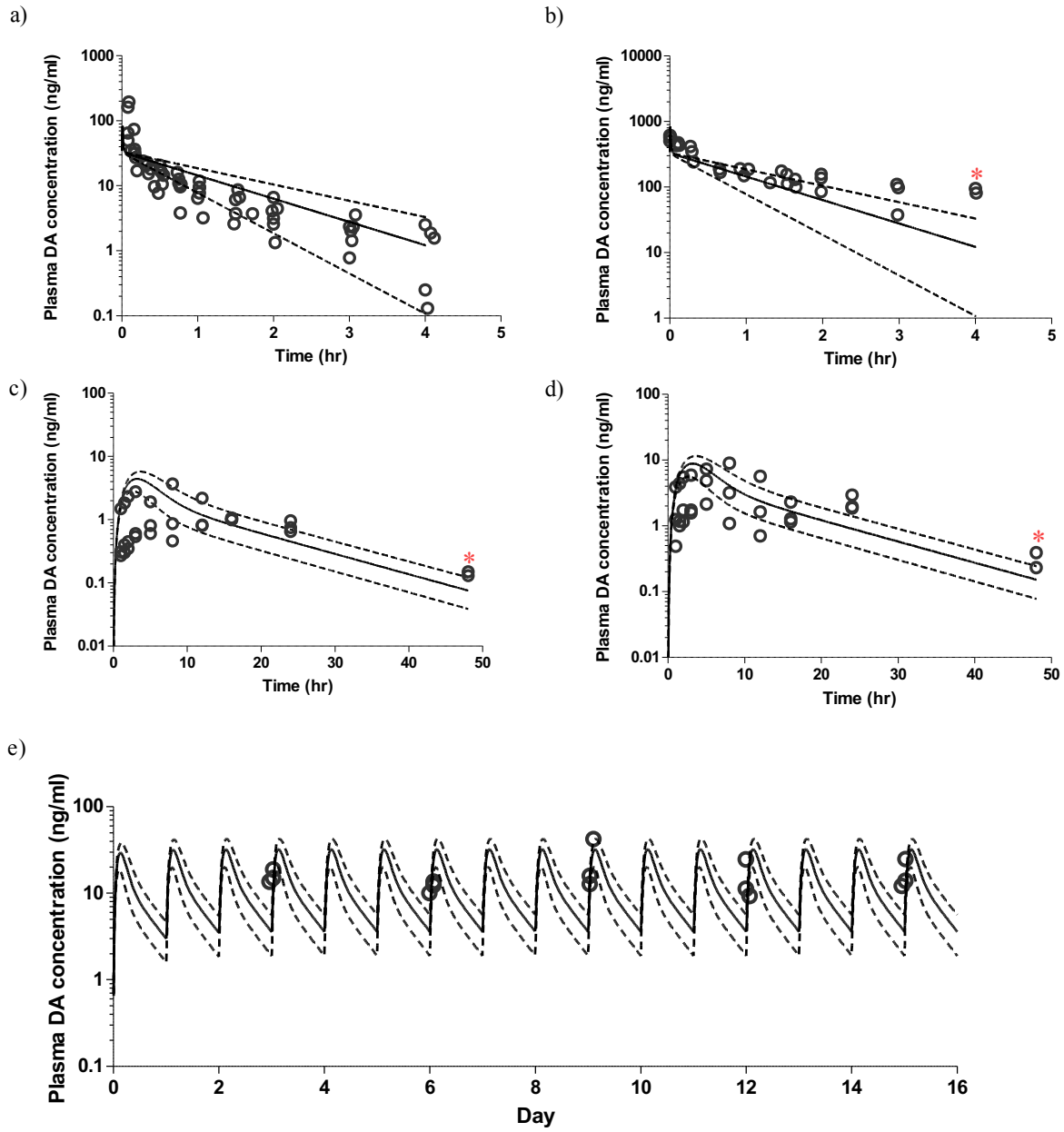


Figure 4.

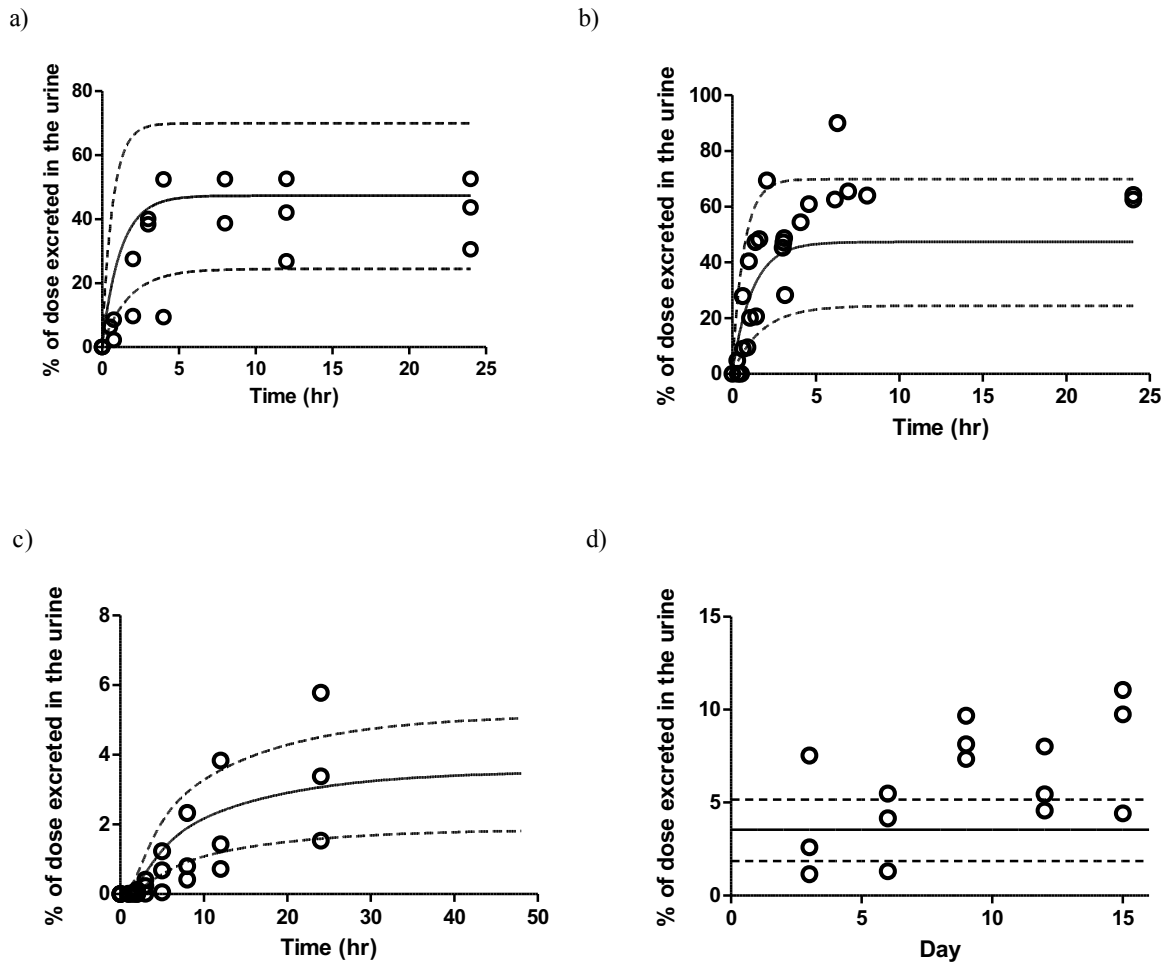
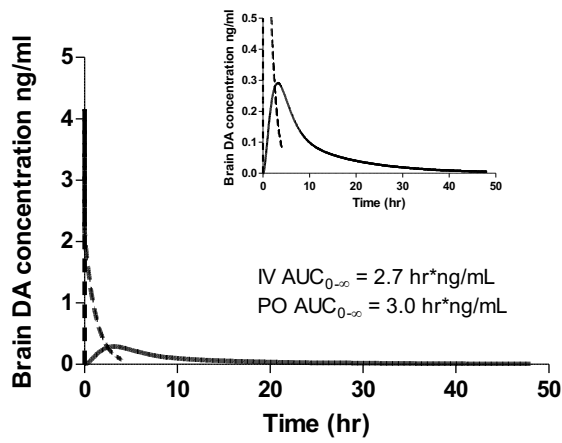
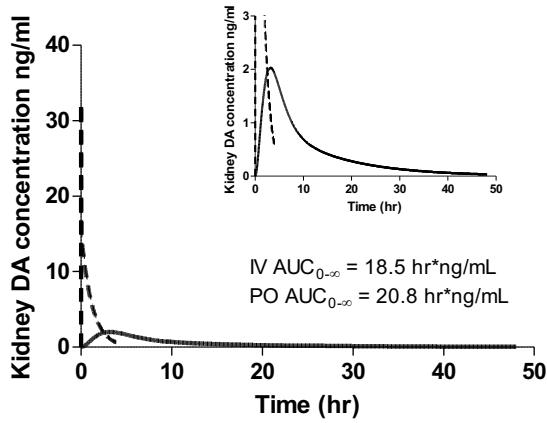


Figure 5.

a)



b)



c)

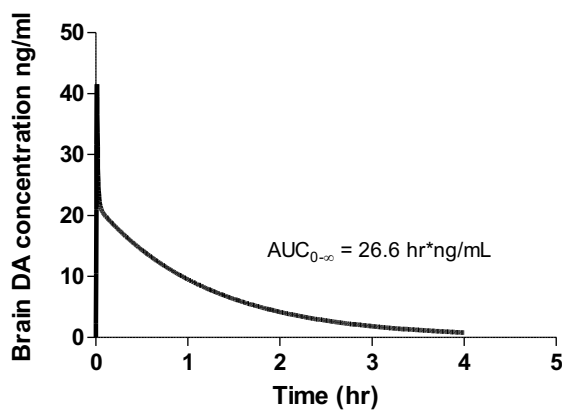


Figure 6.

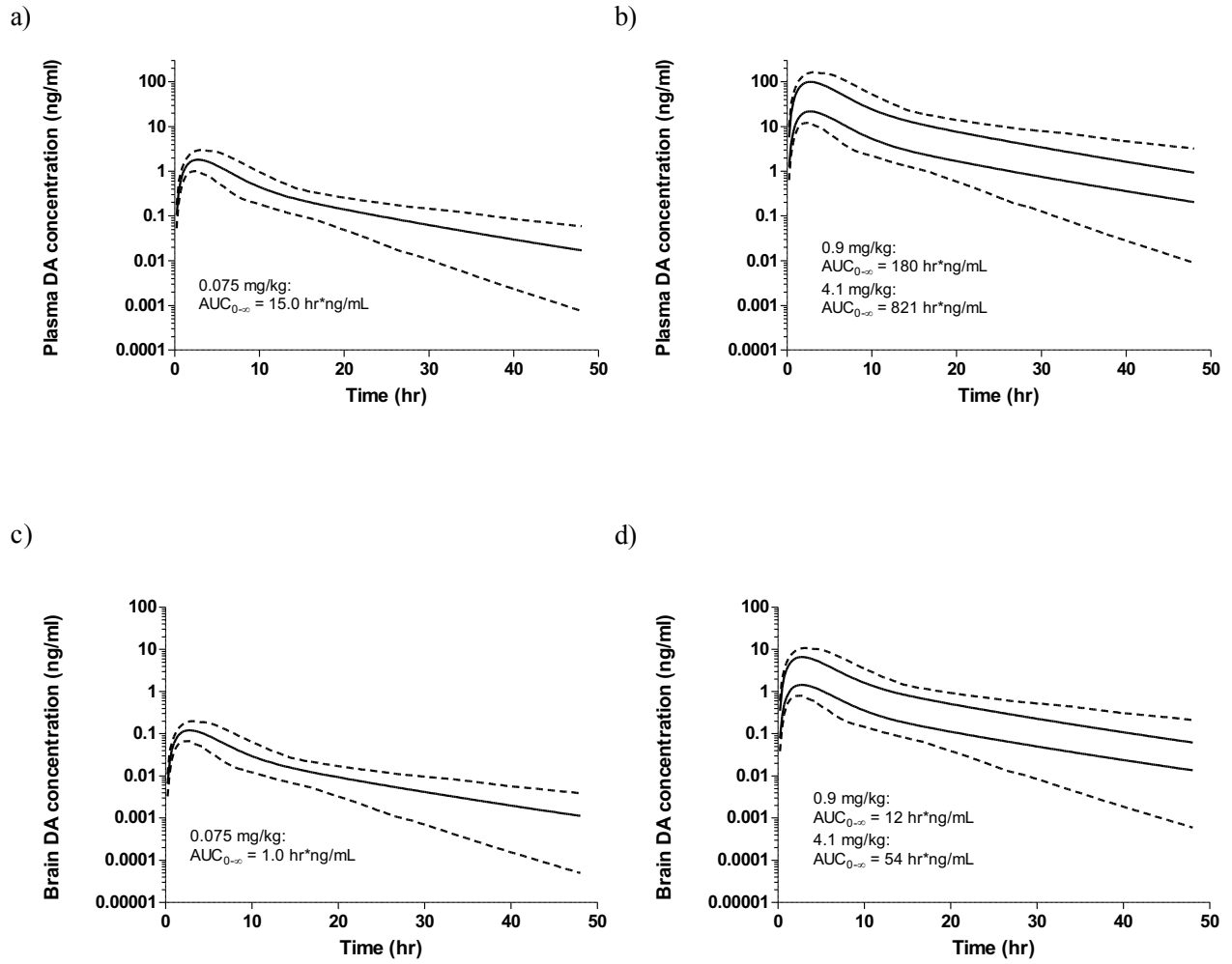


Figure 7.